



# Technical Notes

## Debris Blocker and Flow Terminator for a Shock Tunnel

Ben A. Segall,\*<sup>ⓑ</sup> David Shekhtman,<sup>†</sup> Ahsan Hameed,\*<sup>ⓑ</sup>  
James H. Chen,\* Alex R. Dworzanczyk,\*  
and Nicholas J. Parziale<sup>‡</sup>

Stevens Institute of Technology, Hoboken, New Jersey 07030

<https://doi.org/10.2514/1.J062348>

### I. Introduction

**H**YPERSONIC vehicle design requires an understanding of flow phenomena to predict flow features (e.g., separation bubbles, wakes, and transition) and calculate engineering quantities (e.g., lift, drag, and wall temperature) [1]. Reflected-shock tunnels are one class of ground-test facility that can be used when enthalpy is a consideration in research or design [2]. The primary diaphragm in a reflected-shock tunnel is typically metallic and can produce particulate that gets entrained in the driver gas; this particulate passes through the nozzle after a test and can be abrasive to the wind-tunnel model. This abrasion can alter the surface finish of the model such that boundary-layer studies are compromised. The type of surface instrumentation that can be used is also limited for fear of damage, which is a major reason for interest in nonintrusive optical-based measurement techniques [3].

Researchers have made efforts to address this concern through numerous methods. Hertzberg et al. [4] used a nozzle positioned at an angle away from the shock-tube axial direction, thus using centrifugal force to accelerate particulate out of the flow. Chue and Eitelberg [5] studied the shock-wave/boundary-layer interaction in the reservoir of the High Enthalpy Shock Tunnel Göttingen (HEG) shock tunnel [6]. That work focused on the flow structure around a cylindrical plate positioned near the nozzle throat that acts as a “particle stopper.” Holden [7] and Holden and Parker [8] described a method in the Large Energy National Shock Tunnel (LENS) tunnels where the flow was terminated after the test time by a “fast-acting valve” that closed the nozzle throat to protect the models and the throat from thermal or mechanical damage. Additionally, this valve can prevent overpressurizing the dump tank with the high-pressure driver gas after a test. Lee et al. discussed a design/experimentation study of a “stationary throat plug” [9,10] in addition to a “moving throat plug” [11] in the Korea Advanced Institute of Science and Technology (KAIST) shock tunnel. Hornung and Parziale [12] explored introducing a “blocker” near the nozzle throat of the T5 reflected-shock tunnel [13] to reduce particle impact on a model, as others have done,

but also reduce freestream disturbances by disrupting the focusing of the radially propagating shock wave during tunnel startup.

In this work, we discuss a simple nozzle centerbody that functions as a debris blocker and a flow terminator. The body is a 101.6-mm- (4-in.)-diameter neoprene rubber ball that is suspended near the shock-tube endwall. The plugging action occurs when the ball is advected into the shock-tunnel throat insert following the useful test time. Pitot- and static-pressure results are presented that show that the run condition is not compromised and the flow quality is improved when a centerbody is used. Using the *t*-test method, we determined there to be a statistically significant 12% reduction in the Pitot-pressure fluctuations with the addition of the centerbody.

### II. Stevens Shock Tunnel

The Stevens Shock Tunnel (SST) is a facility designed to replicate Mach 6 flow conditions with an enthalpy of  $\approx 1.5$  MJ/kg and a unit Reynolds number  $0.10\text{--}10 \times 10^6 \text{ m}^{-1}$  for at least 4 ms. The facility can also be run at low-enthalpy/cold-flow conditions to provide high Reynolds numbers and longer test times (greater than  $35 \times 10^6 \text{ m}^{-1}$  for at least 15 ms). In Fig. 1, the current configuration of the tunnel is displayed. The driver section is 5.0 m (16.4 ft) long, and the driven section is 11.1 m (36.3 ft) long. A double-diaphragm section is used to initiate a tunnel experiment in the current test series. More details on the design and performance of the Stevens Shock Tunnel can be found in the work of Shekhtman et al. [14]. In this work, helium is used as the driver gas, and air is used as the driven gas.

As shown in Fig. 2, the centerbody is a 101.6-mm- (4-in.)-diameter neoprene rubber ball positioned along the centerline such that one side of the ball is positioned nearly tangential to the shock-tube endwall. The 800 g (1.76 lb) ball must travel a short distance of approximately 31.8 mm (1.25 in.) until it first makes contact with the throat insert to plug it, forming a seal just upstream of the area minimum; the throat diameter is 51.27 mm (2.018 in.). The material of neoprene was chosen because of its cost, sealing characteristics, elasticity (kept its form sealing against the copper-throat insert), hardness relative to the throat insert, and observed resistance to ablation. The ball was sourced from Wilden (part no. 15-1085-51), and it is typically used as a component in a large valve. For scale, in Fig. 2, the inner diameter of the shock tube is 193.7 mm (7.625 in.), the centerbody diameter is 101.6 mm (4 in.), and the throat diameter is 51.27 mm (2.018 in.). The copper-throat insert is shown as copper in color.

Placing an obstruction in the reservoir of the shock tunnel has the potential to disturb test gas as it flows from the reservoir, over the obstruction (the ball), through the throat, and into the nozzle. The blockage-area ratio of the ball with respect to the pipe wall is  $A_{\text{ball}}/A_{\text{tube}} = 0.275$  because the inner diameter of the shock tube is 193.7 mm (7.625 in.). We estimated that this blockage area was acceptably low because it increased the Mach number in the reservoir when the test slug was draining from  $M = 0.04$  (without the ball) to  $M = 0.14$  (with the ball), assuming an inviscid, calorically perfect gas. That is, the size of the ball would be large enough to block particulate from the primary diaphragm ( $A_{\text{ball}}/A_{\text{throat}} = 3.93$ ) but small enough so as not to excessively increase the Mach number in the reservoir. The literature suggests the freestream disturbance level is affected by the Mach number in the reservoir [15,16].

The ball is suspended by a compliant Viton® rubber o ring of 3.53 mm (0.139 in.) in width, which serves as a pendulum chord. A 6.35-mm- (0.25-in.)-diameter hole was drilled into the ball for the o ring. The hole is oriented vertically such that the o ring is outside the contact surface between the ball and the copper insert. Both the neoprene and Viton were observed to endure reservoir conditions of up to 1800 K; a photograph of the ball is shown in Fig. 3, and there are no visible signs of deterioration after approximately 75 shots as of this writing.

Presented as Paper 2022-1402 at the AIAA SciTech 2022 Conference, San Diego, CA, January 3–7, 2022; received 17 August 2022; revision received 24 February 2023; accepted for publication 1 March 2023; published online 22 March 2023. Copyright © 2023 by the authors. Published by the American Institute of Aeronautics and Astronautics, Inc., with permission. All requests for copying and permission to reprint should be submitted to CCC at [www.copyright.com](http://www.copyright.com); employ the eISSN 1533-385X to initiate your request. See also AIAA Rights and Permissions [www.aiaa.org/randp](http://www.aiaa.org/randp).

\*Graduate Student, Mechanical Engineering, Castle Point on Hudson.

<sup>†</sup>Postdoctoral Researcher, Mechanical Engineering, Castle Point on Hudson.

<sup>‡</sup>Associate Professor, Mechanical Engineering, Castle Point on Hudson; [nick.parziale@gmail.com](mailto:nick.parziale@gmail.com). Senior Member AIAA (Corresponding Author).

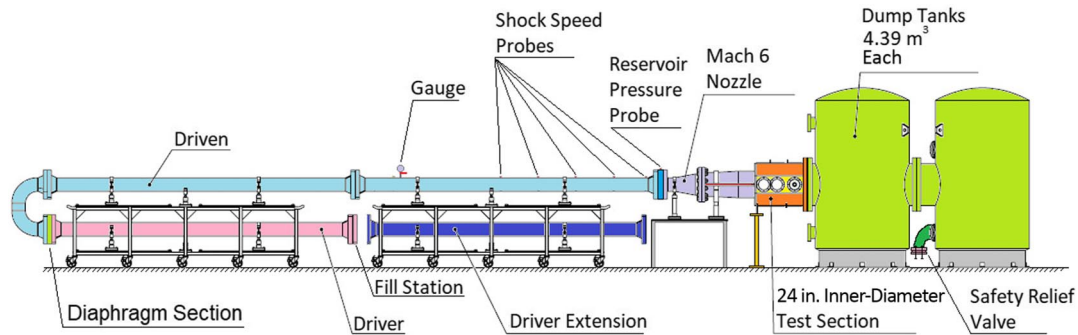


Fig. 1 Schematic of Stevens Shock Tunnel.

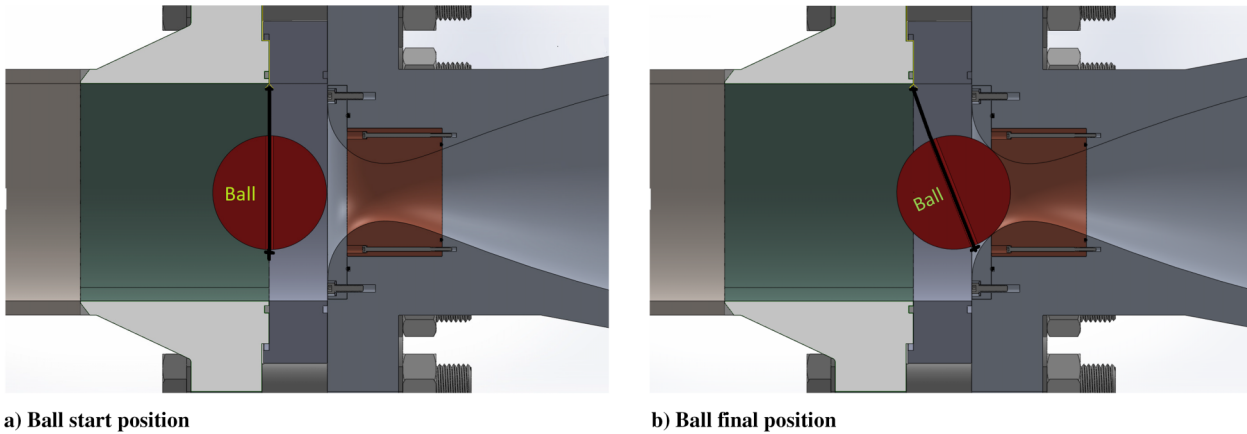


Fig. 2 Schematic of ball plugging the nozzle converging section. The ball moves from the position in Fig. 2a to that in Fig. 2b.

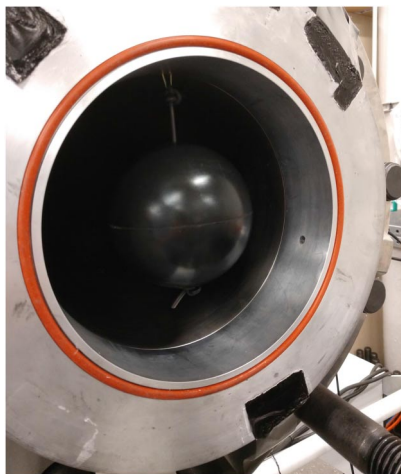


Fig. 3 Photograph of nozzle centerbody looking upstream at the shock-tube end.

### III. Performance of the Nozzle Centerbody

The ball serves as a diaphragm-debris blocker and a nozzle-flow terminator. The effect of the ball as a debris blocker is shown in Fig. 4. The run conditions are listed in Table 1. (In Table 1,  $P_4$  is the driver-section pressure;  $P_4/P_1$  is the driver-to-driven pressure ratio that determines the driven air pressure  $P_1$ ;  $u_s$  is the shock speed;  $M_s$  is the shock Mach number;  $T_R$  is the reservoir temperature;  $P_R$  is the reservoir pressure;  $h_R$  is the reservoir enthalpy;  $T_\infty$  is the freestream temperature;  $M_\infty$  is the freestream Mach number; and  $Re_\infty^u$  is the unit Reynolds number.) The camera settings were consistent for all shots. The lights in the laboratory were turned off for shot 179, resulting in a different contrast. The frames are presented for the time we considered to be the steady test time of  $\approx 3\text{--}8$  ms in Fig. 5. The secondary

diaphragm is placed at the nozzle throat and is a  $76\text{-}\mu\text{m}$ - ( $0.003\text{-in.}$ )-thick 1100-O aluminum-foil sheet for all experiments. This thin foil sheet is ruptured and then advected past the field of view before the test time begins (before 2 ms), and so the particulate in Fig. 4 is not from the secondary diaphragm. Oscillations are present in the Pitot- and static-pressure measurements before 3 ms, which correspond to the secondary diaphragm advection and general startup period (Fig. 5). The ball assists in keeping the test section free of debris during the run, which is critical to boundary-layer instability, transition to turbulence experiments, and preservation of the test-article surface (surface finish and coatings). Additionally, the ball protects the nozzle throat from being damaged by flying debris. Sources of debris include the ruptured primary diaphragm and particulate left over from previous experiments, which coat the surfaces of the shock tunnel and can increase the facility disturbance level [17–19]. In the Stevens Shock Tunnel, cleaning of the shock tube is done via a motorized cart that pushes out large debris and lay a Kevlar® line from which to pull through a cylindrical sponge strapped with a microfiber cloth on its circumferential surface. Additionally, the nozzle throat and nozzle are cleaned before each run.

In addition to serving as a debris blocker, the ball can behave as a high-speed valve, which can cut flow through a nozzle, reducing run recoil and forces on a facility. In Fig. 6, we show the static pressure in the test section. The run conditions are listed in Table 1. Following the useful test time (3–8 ms, marked as “Test Time”), there is a period where the driver gas flows into the test section increasing the static pressure. This increase in pressure ceases when the ball seals against the copper-throat insert, and it takes place in approximately 40–100 ms. For comparison, the pressure trace for shot 179, which did not use the centerbody, demonstrates the rising tank pressure until stabilization at 73.7 kPa (10.7 psia). For driver pressures appreciably higher than that for shot 179, test-section overpressurization could potentially occur without the centerbody; its use, along with a pressure-relief valve, ensures safe operation.

In general, we observed that the Pitot- and static-pressure traces were steadier for a longer period of time when a centerbody was used.

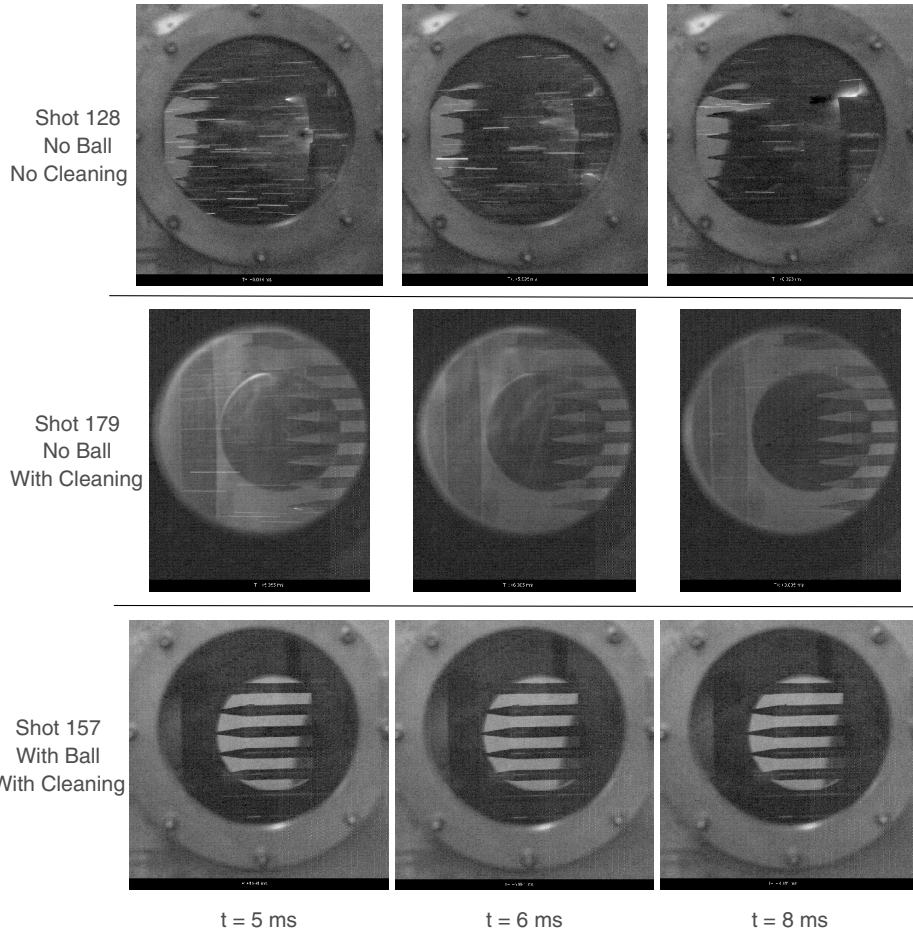


**Fig. 4** Effect of tunnel cleaning procedures and centerbody apparatus on debris entering the test section. The useful test time is from approximately 4 to 9 ms.

**Table 1** Run conditions: driven gas is air for all shots except 157, which was 99% N<sub>2</sub>/1% Kr

Shot	Driver gas	$P_4$ , MPa	$P_4/P_1$	$P_R/P_4$	$u_s$ , m/s	$M_s$	$P_R$ , MPa	$T_R$ , K	$h_R$ , MJ/kg	$T_\infty$ , K	$M_\infty$	$Re_\infty^\mu$ 10 <sup>6</sup> , 1/m	Ball <sup>a</sup>
110	He	3.44	130	0.72	1220	3.51	2.48	1713	1.62	249	5.77	2.66	N
111	He	3.44	129	0.70	1220	3.51	2.41	1700	1.60	246	5.78	2.61	N
112	He	3.43	120	0.73	1219	3.51	2.50	1686	1.58	244	5.77	2.76	N
128	He	1.88	155	0.76	1240	3.58	1.42	1830	1.77	272	6.04	1.6	N
146	He	3.47	131	0.68	1270	5.74	2.35	1758	1.68	258	5.88	2.4	N
157	He	3.17	96	0.76	1200	3.17	2.42	1610	1.48	222	5.63	2.4	Y
169	He	3.58	114	0.74	1220	3.51	2.67	1670	1.57	240	5.83	3.0	Y
179	He	3.93	125	0.74	1240	3.58	2.93	1740	1.66	252	5.60	3.3	N
180	He	1.21	120	0.71	1200	3.44	0.859	1650	1.54	238	6.05	0.94	Y
181	He	3.47	121	0.69	1220	3.51	2.40	1670	1.56	239	5.89	3.1	Y
182	He	5.29	115	0.71	1220	3.77	2.40	1660	1.56	237	5.83	4.6	Y
183	He	6.99	115	0.73	1200	3.44	5.09	1640	1.53	232	5.94	5.3	Y
186	He	3.55	110	0.73	1195	3.44	2.64	1627	1.51	231	5.86	3.0	Y

<sup>a</sup>The “Ball” column indicates the use of a centerbody, where Y or N denote yes or no, respectively.

In a comparison of four shots without the ball (shots 110, 111, 112, and 179) and four shots with the ball (shots 146, 169, 181, and 186), for which the run conditions are listed in Table 1, a 12% difference in the root mean square of the Pitot-pressure fluctuation  $P'_{Pitot}$  was observed in the last 2 ms of the steady test time. We analyzed the last 2 ms of test time because that was when we typically observed larger  $P'_{Pitot}$  and when one would typically expect driver-gas contamination to be problematic. A  $t$  test in MATLAB was performed for the following null hypothesis: the introduction of the centerbody does not influence pressure fluctuations during the last 2 ms of test time. The null hypothesis was rejected with a 95% confidence interval; that is, the 12% reduction in  $P'_{Pitot}$  with the addition of the centerbody is statistically significant.

In Fig. 5, the reservoir, static-, and Pitot-pressure traces are presented for two different shock-tunnel configurations, with and without the centerbody. For both runs, the usable test time of  $\approx 3\text{--}8$  ms is denoted by the yellow-highlighted regions. Shot 169, during which the centerbody was used, resulted in steadier, longer pressure traces than for shot 179, where the centerbody was not used. This notable difference in pressure-trace behavior was consistent among several runs considered in the aforementioned comparison that did and did not use the ball.

We observe that a sudden static-pressure decrease for shot 179 coincides with oscillations in the Pitot pressure. We hypothesize that this could be an indication of driver-gas contamination due to either bifurcation [20,21] or test-gas slug depletion [22]. Attributing the

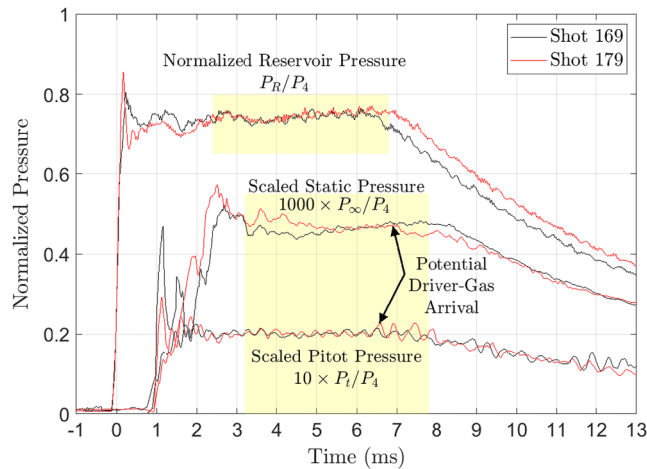


**Fig. 5 Shock-tunnel pressure traces for shots 169 (with centerbody) and 179 (without centerbody). Test times are denoted by yellow highlighted regions.**

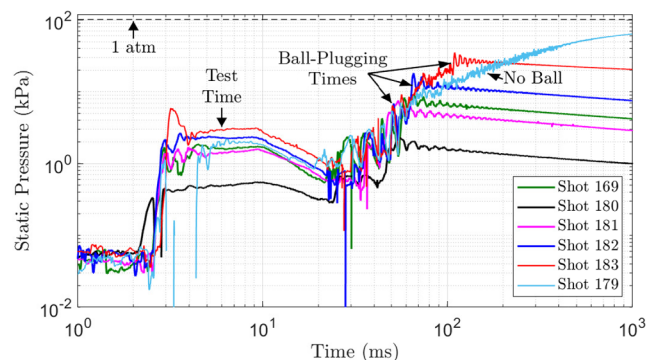


**Fig. 6 Static-pressure traces for multiple shots showing test intervals and ball-plugging times. Shot 179 does not use the centerbody.**

drop in static pressure and the increase in fluctuations to driver-gas contamination is speculation; to confirm this, we would need to make observations of the helium mass fraction as in Ref. [23] or Ref. [24] and consider this as future work. However, static-pressure decrease is known to serve as an indication of driver-gas contamination [25,26]. This is because the ratio of specific heat increases, increasing the Mach number and further expanding the gas for nominally the same area ratio. Because of competing effects, the mean Pitot pressure is not as drastically affected. The results of a sample calculation illustrating the change of the static and Pitot pressures due to the increasing fraction of helium (He) are presented in Fig. 7. For this calculation, we assume the area ratio is unchanged and the gas is calorically perfect. Figure 7 shows that the static pressure is more affected than the Pitot pressure. The driving mechanism behind this observed difference in steadiness with and without the ball could be the centerbody interdicting the vortex structures found to facilitate driver-gas contamination, as noted in the works of Chue et al. [22] and Goozée et al. [27]; this could be a topic of future research.

#### IV. Conclusions

In the Stevens Shock Tunnel, a nozzle centerbody is used as a diaphragm-debris blocker and nozzle-flow terminator. Since the introduction of the ball into the SST, no wear on the copper-throat insert and test-article surfaces has been observed. Additionally, high-speed nozzle-flow termination reduced facility recoil at the end of an experiment and prevents test-section and dump-tank overpressurization. Plugging the flow following the useful test time creates an opportunity to reclaim the driver gas that, which in the present experiments, was helium. A cost/benefit analysis will be performed to assess the viability of the driver-gas reclamation process. It was observed that the Pitot- and static-pressure traces were consistently

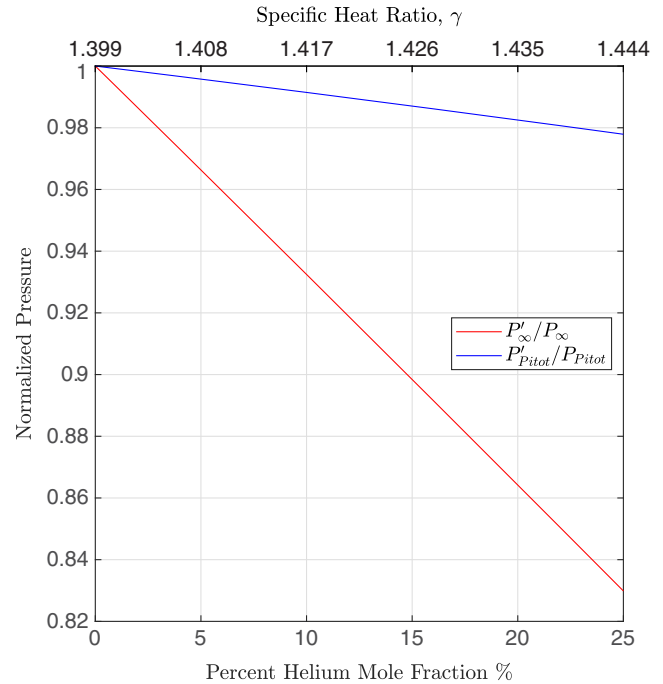


**Fig. 7 Variation of static and Pitot pressures with respect to percent mole fraction of helium in a Mach 6 air freestream.**

steadier for a longer period of time when a centerbody was used. Using the  $t$ -test method, this was determined to be a statistically significant 12% reduction in the Pitot-pressure fluctuations with the addition of the centerbody. It is speculated that this could be an indication that the centerbody reduces driver-gas contamination due to bifurcation or test-gas slug depletion; alternatively, this could be an indication that the geometry change in the reservoir altered the propagation of noise in the facility. Investigation of the fundamental mechanisms behind this behavior is a topic of future work. The ball has performed well for approximately 75 shots in the SST with no observed wear at reservoir conditions typically above  $T_R = 1600$  K; however, other researchers may require a centerbody that could withstand more demanding test conditions. The use of a spherical centerbody in more demanding facilities would require identifying the conditions where neoprene would begin to degrade; alternatively, a soft metal, like copper, could be used.

#### Acknowledgments

Ben A. Segall, David Shekhtman, Ahsan Hameed, James H. Chen, Alex R. Dworzanczyk, and Nicholaus J. Parziale were supported by U.S. Office of Naval Research and U.S. Air Force Office of Scientific Research (AFOSR) grants, including N00014-19-1-2523, N00014-20-1-2637, N00014-20-1-2682, N00014-20-1-2549, FA9550-18-1-0403, and FA9550-19-1-0182. We thank Eric Marineau and the U.S. Office of Naval Research for sponsoring the construction and development of the Stevens Shock Tunnel. We also thank AFOSR Program Manager Sarah Popkin for her support.

#### References

- [1] Leyva, I. A., "The Relentless Pursuit of Hypersonic Flight," *Physics Today*, Vol. 70, No. 11, 2017, pp. 30–36. <https://doi.org/10.1063/PT.3.3762>
- [2] Hannemann, K., "Short-Duration Testing of High Enthalpy, High Pressure, Hypersonic Flows," *Springer Handbook of Experimental Fluid Mechanics*, edited by C. Tropea, A. L. Yarin, and J. F. Foss, Springer, New York, 2007, pp. 1081–1125.
- [3] Danehy, P. M., Weisberger, J., Johansen, C., Reese, D., Fahringer, T., Parziale, N. J., Dedic, C., Estevadeordal, J., and Cruden, B. A., "Non-Intrusive Measurement Techniques for Flow Characterization of Hypersonic Wind Tunnels," Flow Characterization and Modeling of Hypersonic Wind Tunnels (NATO Science and Technology Organization Lecture

- Series STO-AVT 325), von Kármán Inst. NF1676L-31725, Brussels, Belgium, 2018, <https://ntrs.nasa.gov/citations/20190029251>.
- [4] Hertzberg, A., Wittliff, C. E., and Hall, J. G., "Summary of Shock Tunnel Development and its Application to Hypersonic Research," U.S. Air Force Office of Scientific Research TR 60-139, Arlington, VA, 1961.
- [5] Chue, R. S. M., and Eitelberg, G., "Studies of the Transient Flows in High Enthalpy Shock Tunnels," *Experiments in Fluids*, Vol. 25, Nos. 5–6, 1998, pp. 474–486. <https://doi.org/10.1007/s003480050253>
- [6] Hanneman, K., and Beck, W. H., "Aerothermodynamics Research in the DLR High Enthalpy Shock Tunnel HEG," *Advanced Hypersonic Test Facilities*, AIAA, Reston, VA, 2002, pp. 205–238. <https://doi.org/10.2514/5.9781600866678.0205.0237>
- [7] Holden, M. S., "Development and Code Evaluation Studies in Hypervelocity Flows in the LENS Facility," *Proceedings of the 2nd European Symposium on Aerodynamics for Space Vehicles*, European Space Agency, ESTEC, Paris, Noordwijk, The Netherlands, 1994, pp. 319–334.
- [8] Holden, M. S., and Parker, R. A., "LENS Hypervelocity Tunnels and Application to Vehicle Testing at Duplicated Flight Conditions," *Advanced Hypersonic Test Facilities*, AIAA, Reston, VA, 2002, pp. 73–110. <https://doi.org/10.2514/5.9781600866678.0073.0110>
- [9] Lee, J. K., Park, C., and Kwon, O. J., "Experimental Study of Shock Tunnel Flow with a Stationary Throat Plug," *Shock Waves*, Vol. 22, July 2012, pp. 295–305. <https://doi.org/10.1007/s00193-012-0370-2>
- [10] Lee, J. K., Park, C., and Kwon, O. J., "Experimental and Numerical Study of Stationary Throat Plug in Shock Tunnel," *Journal of Thermophysics and Heat Transfer*, Vol. 29, No. 3, 2015, pp. 482–495. <https://doi.org/10.2514/1.T4084>
- [11] Lee, J. K., Park, C., and Kwon, O. J., "Experimental Study of Moving Throat Plug in a Shock Tunnel," *Shock Waves*, Vol. 25, July 2015, pp. 431–442. <https://doi.org/10.1007/s00193-015-0573-4>
- [12] Hornung, H. G., and Parziale, N. J., "Reflected Shock Tunnel Noise Control," *Proceedings of the 15th International Conference on the Methods of Aerophysical Research*, Akademgorodok, Novosibirsk, Russia, 2010.
- [13] Hornung, H. G., "Performance Data of the New Free-Piston Shock Tunnel at GALCIT," *Proceedings of 17th AIAA Aerospace Ground Testing Conference*, AIAA Paper 1992-3943, 1992. <https://doi.org/10.2514/6.1992-3943>
- [14] Shekhtman, D., Hameed, A., Segall, B. A., Dworzanczyk, A. R., and Parziale, N. J., "Initial Shakedown Testing of the Stevens Shock Tunnel," *Proceedings of AIAA SciTech 2022*, AIAA Paper 2022-1402, 2022. <https://doi.org/10.2514/6.2022-1402>
- [15] Laufer, J., "Some Statistical Properties of the Pressure Field Radiated by a Turbulent Boundary Layer," *Physics of Fluids (1958–1988)*, Vol. 7, No. 8, 1964, pp. 1191–1197. <https://doi.org/10.1063/1.1711360>
- [16] Schneider, S. P., "Development of Hypersonic Quiet Tunnels," *Journal of Spacecraft and Rockets*, Vol. 45, No. 4, 2008, pp. 641–664. <https://doi.org/10.2514/1.34489>
- [17] Parziale, N. J., Shepherd, J. E., and Hornung, H. G., "Free-Stream Density Perturbations in a Reflected-Shock Tunnel," *Experiments in Fluids*, Vol. 55, No. 2, 2014, Paper 1665. <https://doi.org/10.1007/s00348-014-1665-0>
- [18] Parziale, N. J., Jewell, J. S., Leyva, I. A., and Shepherd, J. E., "Effects of Shock-Tube Cleanliness on Slender-Body Hypersonic Instability and Transition Studies at High-Enthalpy," *Proceedings of AIAA SciTech 2015*, AIAA Paper 2015-1786, 2015. <https://doi.org/10.2514/6.2015-1786>
- [19] Jewell, J. S., Parziale, N. J., Leyva, I. A., and Shepherd, J. E., "Effects of Shock-Tube Cleanliness on Hypersonic Boundary Layer Transition at High Enthalpy," *AIAA Journal*, Vol. 55, No. 1, 2017, pp. 332–338. <https://doi.org/10.2514/1.J054897>
- [20] Davies, L., "The Interaction of the Reflected Shock with the Boundary Layer in a Shock Tube. Part 1," Her Majesty's Stationary Office, Ministry of Aviation: Aeronautic Research Council CP-880, London, July 1966.
- [21] Davies, L., and Wilson, J. L., "Influence of Reflected Shock and Boundary-Layer Interaction on Shock-Tube Flows," *Physics of Fluids*, Vol. 12, No. 5, 1969, Paper 137. <https://doi.org/10.1063/1.1692625>
- [22] Chue, R. S. M., Tsai, C. Y., and Bakos, R. J., "Driver Gas Contamination in a Detonation-Driven Reflected-Shock Tunnel," *Shock Waves*, Vol. 13, March 2003, pp. 367–380. <https://doi.org/10.1007/s00193-003-0221-2>
- [23] Sudani, N., and Hornung, H. G., "Gasdynamical Detectors of Driver Gas Contamination in a High-Enthalpy Shock Tunnel," *AIAA Journal*, Vol. 36, No. 3, 1998, pp. 313–319. <https://doi.org/10.2514/2.383>
- [24] Sudani, N., Valiferdowski, B., and Hornung, H. G., "Test Time Increase by Delaying Driver Gas Contamination for Reflected Shock Tunnels," *AIAA Journal*, Vol. 38, No. 9, 2000, pp. 1497–1503. <https://doi.org/10.2514/2.1138>
- [25] Hannemann, K., Schneider, M., Reimann, B., and Schramm, J. M., "The Influence and Delay of Driver Gas Contamination in HEG," *21st AIAA Aerodynamic Measurement Technology and Ground Testing Conference*, AIAA Paper 2000-2593, 2000, pp. 1–14. <https://doi.org/10.2514/6.2000-2593>
- [26] Olivier, H., "The Aachen Shock Tunnel TH2 with Dual Driver Mode Operation," *Experimental Methods of Shock Wave Research*, Springer, New York, 2016, pp. 111–129. [https://doi.org/10.1007/978-3-319-23745-9\\_5](https://doi.org/10.1007/978-3-319-23745-9_5)
- [27] Goozée, R. J., Seal, P. A., and Saxena, D. R., "Simulation of a Complete Reflected Shock Tunnel Showing a Vortex Mechanism for Flow Contamination," *Shock Waves*, Vol. 15, Nos. 3–4, 2006, pp. 165–176. <https://doi.org/10.1007/s00193-006-0015-4>

C. Lee  
Associate Editor